

Mass Transfer Effects for Uniform and Nonuniform Catalyst Pellets

KISHOR PATEL AND J. M. SMITH

University of California, Davis, California 95616

Received June 13, 1975

Reaction rates for the catalytic oxidation of hydrogen in a spherical, single-pellet, recycle reactor system showed negligible external mass transfer resistances at Reynolds numbers as low as 0.27. Only at lower flow rates, where complete mixing of gas in the reactor space was doubtful, did fluid-to-pellet mass transfer affect the rate in this particular reactor arrangement. Pellets prepared with a nonuniform distribution of active catalyst particles, and an accompanying two-thirds reduction in mass transfer surface, also exhibited no external diffusion resistance in the temperature range 94–180°C, unless Re was less than 0.27. However, at lower Reynolds numbers the retardation of the rate by mass transfer was greater for the nonuniform pellets.

NOMENCLATURE

a_m	external area of catalyst pellet, $\text{cm}^2/(\text{g of undiluted catalyst})$	Q	sure of oxygen in pellet reactor recirculation rate (total flow rate, see Fig. 1) through reactor, cm^3/min at 25°C, 1 atm
C_{O_2}	oxygen concentration, g moles/ cm^3	R_g	gas constant, $\text{cm}^3 \text{ atm}/(\text{g mole})(^\circ\text{K})$
D_e	effective diffusivity of oxygen in the pellet, cm^2/sec	R_o	radius of pellet, cm
D_{O_2, H_2}	molecular diffusivity, cm^2/sec	r	rate of production of water, g moles/(sec)(g), r_∞ = rate corresponding to no external diffusion resistance; r_Q = rate at a recirculation rate of Q
$(\bar{D}_K)_{O_2}$	Knudsen diffusivity at average macropore diameter, cm^2/sec	T	temperature, °K
\bar{D}	average composite diffusivity of oxygen in the macropores of the pellet, cm^2/sec	y	mole fraction oxygen
d_p	pellet diameter, cm	α	thermal diffusivity of catalyst pellet, $k_e C_p / \rho$, cm^2/sec
E	activation energy, cal/g mole	β_s	dimensionless group defined by Eq. (4)
F_t	feed rate to the reactor, cm^3/sec at 25°C, 1 atm	ϵ_m	macropore porosity
ΔH	enthalpy change of reaction per mole of oxygen, cal/g mole	δ	tortuosity factor, defined by Eq. (6)
k_e	effective thermal conductivity	ρ_c	mass of active catalyst particles per volume of pellet, g/cm^3
k_m	mass transfer coefficient between bulk gas in reactor and pellet surface, cm/sec	ϕ_s	dimensionless group defined by Eq. (5)
m_c	mass of active catalyst particles per pellet, g	γ_s	dimensionless group defined by Eq. (3)
\bar{p}_{O_2}	average partial pressure of oxygen in differential, particle reactor, atm; p_{O_2} = partial pres-		

η effectiveness factor of catalyst pellet

Subscripts

a macropores
 b bulk
 i feed condition or micropores
 o outlet condition
 Q at recirculation rate Q
 s surface of pellet.

INTRODUCTION

Maymo and Smith (2) found that a reactor consisting of a relatively large catalyst pellet centered in a small spherical vessel, and operated at high recycle rate, provided a useful arrangement for studying intraparticle transport processes. Since data for mass transfer coefficients between bulk gas and pellet are unavailable for this type of reactor, the system has recently been operated over a range of recycle rates. This communication reports the results of this new study and also reaction rates for nonuniform distribution of active catalyst in the pellet. The latter question has become of interest in view of the observations of Moffat *et al.* (3) on the disproportionation of propylene. These authors found that the conversion in a fixed bed increased with increased flow rate. Such evidence of gas-particle mass transfer resistance contradicted calculations based upon available mass transfer coefficients and upon using the entire outer surface of the catalyst particles as the area for mass transfer. The difference between calculated and observed mass transfer rates was too great to be explainable by errors in mass transfer coefficients. It was suggested that the effective surface for mass transfer may be less than the total outer surface because of a low concentration of very active catalyst sites.

In the data reported here a decreased mass transfer area was obtained by arbitrarily locating platinum-on-alumina catalyst particles in one part of a pellet. Rates

of oxidation of hydrogen were measured at atmospheric pressure for such nonuniform pellets and compared with data for pellets containing uniformly distributed catalyst particles. The effect of recycle flow rate was studied with the same pellets.

APPARATUS AND EXPERIMENTS

The oxidation of hydrogen, with a uniformly distributed platinum-on-alumina catalyst, in a single-pellet recycle reactor was used by Maymo and Smith (2) to investigate intraparticle transport resistances. The same apparatus, which consisted of a single 1.92-cm pellet centrally mounted in a 9.0-cm spherical chamber, was used in the present study.¹ Tangential introduction of the feed and partial recycling of the product gases resulted in a swirling motion of the reaction mixture around the catalyst pellet. The reactor and recycle arrangement are shown in Fig. 1. Purified hydrogen and oxygen at controlled rates were fed to the reactor and the oxygen content of the effluent was determined in a thermal conductivity cell.

Catalyst particles containing 0.02 wt % platinum were prepared by soaking alumina particles (61–175 μm size range) in a dilute solution of chloroplatinic acid. The particles were then dried, heated in air at 550°C to decompose the chloroplatinic acid, and reduced with hydrogen at 300°C for 3 hr. The procedure is described in detail by Maymo and Smith (2). The properties of the alumina particles (from American Cyanamid Co.) are given in Table 1.

All of the pellets contained 0.3 g of the 0.02 wt % Pt catalyst particles and 1.9 g of pure alumina particles of the same size range (61–175 μm). For the uniform pellets the catalyst was mixed homogeneously with the 1.9 g of alumina particles

¹ A flow diagram of the entire apparatus as well as drawings of the reactor and construction details are given by Maymo and Smith (2).

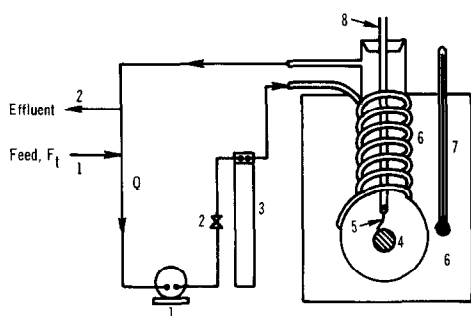


FIG. 1. Pellet reactor: 1, Diaphragm pump. 2, Flow controllers. 3, Manometers. 4, Catalyst pellet. 5, Pellet support. 6, Constant temperature bath. 7, Thermometer. 8, Glass rod for wire and pellet support.

and formed into a hemisphere in a pellet press. Then the thermocouples were added and the rest of the material added to form the 1.92-cm spherical pellet. Iron-constantan thermocouples (40 gauge) were located at the pellet center and on the outer, spherical surface. Precautions, such as pressing the lead wires of the surface couple to the outer surface for a length of at least 5 mm, were taken to give reason-

TABLE 1
PROPERTIES OF PARTICLES AND PELLETS

A. Alumina particles			
Particle size range	Average micropore radius	Surface area	Solid phase density
61-175 μm	27 \AA	300 m^2/g	2.68 g/cm^3
B. Pellets			
	Uniform	Nonuniform	
Pellet density, g/cm^3	0.580	0.580	
Micropore porosity, ϵ_i	0.23	0.22	
Macropore porosity, ϵ_a	0.54	0.56	
Average micropore radius, \AA	27	27	
Average macropore radius, \AA	6500	6500	
Catalyst particles, g/pellet	0.3	0.3	
Alumina, g/pellet	1.9	1.9	
Effective thermal conductivity $\text{cal}/(\text{cm})(\text{sec})(^\circ\text{C})$	2.72×10^{-4}		

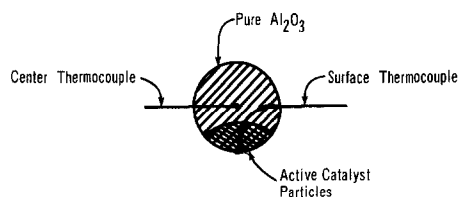


FIG. 2. Nonuniform pellet.

ably reliable temperature readings (4). For the nonuniform pellet the 0.3 g of undiluted catalyst particles were placed about at the bottom of the hemispherical mold and alumina added to complete the hemisphere as indicated in Fig. 2. Pellets made with alumina particles dyed red, instead of with catalyst particles, indicated that the external surface area of the nonuniform pellet was about 30% of the total spherical surface.

PROPERTIES OF PELLETS

The effective thermal conductivity, k_e , of the pellets was estimated by measuring surface and center temperatures as a function of time after the pellet, initially at the uniform temperature of 26°C , was quickly immersed in an air bath maintained at 150°C . The thermal diffusivity, α , was calculated from the temperature difference, ΔT , between surface and center of the pellet using the equations of Carslaw and Jaeger (1). Then k_e was obtained from α using the measured pellet density (Table 1) and $C_p = 0.225 \text{ cal}/(\text{g})(^\circ\text{C})$ for alumina (5).

Mercury porosimeter and pycnometer measurements were made to determine the porosity, density, and pore-volume distribution for the pellets. A summary of these properties is included in Table 1. Three different uniform pellets were prepared in identical fashion. The variation in properties varied from pellet to pellet as follows: ϵ_a from 0.53 to 0.54, ϵ_i from 0.22 to 0.23, and average macropore radius from 5500 to 7000. The average results are shown in Table 1. The macropores represent, approximately, the void space between the catalyst particles in the pellet

and the micropores represent the intraparticle space.

INTRINSIC KINETICS

In order to account for intraparticle and external transport effects, intrinsic rates were measured with catalyst particles (61–175 μm) in a differential (conversion of oxygen < 28%), tubular reactor made of 0.9-cm i.d. Pyrex glass located in a constant-temperature bath. To reduce temperature gradients the bed was prepared with 0.08 g of catalyst particles diluted uniformly with 0.5 g of pure alumina particles and 1.0 g of glass beads (85 μm size). The length of the bed so produced was about 3.0 cm and this was accompanied by 1.5-cm lengths of glass beads before and after the bed. With this arrangement radial and axial temperatures, measured with thermocouples located at four axial positions on the centerline of the reactor and with the bath thermometer, indicated differences from 0.5 to 1.5°C.

Preliminary runs showed that at flow rates (F_t) above about 130 cm^3/min (at 25°C and 1 atm) the reaction rate did not change with flow rate. Accordingly, rates were measured at $F_t = 133 \text{ cm}^3/\text{min}$ and oxygen partial pressures from 0.0037 to 0.015 atmospheres and from 116 to 179°C. Calculations based upon the experimental rate and estimated diffusivities showed

that intraparticle diffusion could not be significant for these small particles. Rates of production of water were calculated from the measured mole fractions of oxygen in the feed (y_i) and exit (y_o) streams and the equation

$$r_\infty = \frac{2F_t(y_i - y_o)o_2}{298(R_g)m_c}, \quad (1)$$

where m_c is the mass of undiluted catalyst particles.

The effects of temperature and oxygen partial pressure on the rate are shown in Figs. 3 and 4 for the two different beds of catalysts that were used. Least-square correlations of the data points give the following equation for the intrinsic rate in g moles/(sec)(g):

$$r_\infty = 0.15(\bar{p}_{O_2})^{0.89} \exp(-5300/R_gT). \quad (2)$$

Similar measurements for catalyst particles prepared in the same way by Maymo and Smith (2) gave an activation energy of 5200 cal/g mole and an order with respect to oxygen of 0.80.

UNIFORM PELLET RESULTS

Effective Diffusivity

Preliminary measurements in the pellet reactor showed that at recirculation rates, Q , of 4000 cm^3/min (25°C, 1 atm) there

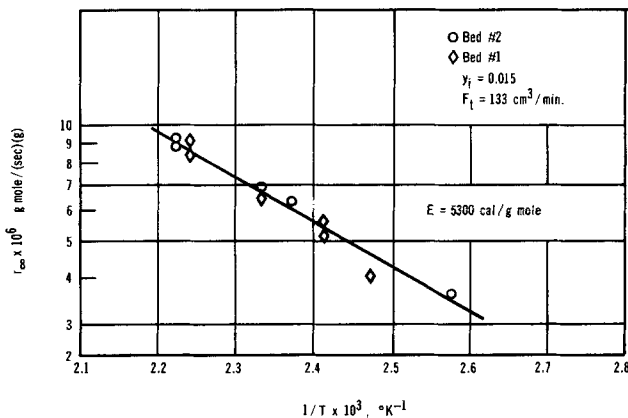


FIG. 3. Arrhenius plot of intrinsic rate data.

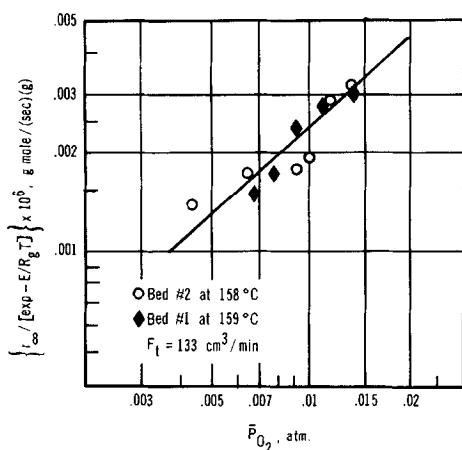


FIG. 4. Effect of oxygen partial pressure on the intrinsic rate.

was no change in observed reaction rate with flow rate. Then rates were determined for three different pellets, all of essentially the same properties, as shown in Table 1. Measured reaction rates and surface temperatures are given in Table 2 for three temperature levels. The reaction rates were determined from the flow rate (F_t) and oxygen analyses using Eq. (1).

These results were then employed with the intrinsic rate expression (Eq. (2)) to evaluate effectiveness factors, η , and the effective diffusivity, D_e , for the uniform pellets. To do this, differential mass and

energy conservation equations for the intraparticle region of the pellet were first solved numerically to determine the effectiveness factor as a function of the dimensionless parameters:

$$\gamma_s = E/R_g T_s, \quad (3)$$

$$\beta_s = \frac{(-\Delta H) D_e (C_{O_2})_s}{k_e T_s}, \quad (4)$$

$$\phi_s = R_o \left(\frac{r_s \rho_c}{2 D_e (C_{O_2})_s} \right)^{1/2}, \quad (5)$$

where $C_{O_2} = p_{O_2}/R_g T$.

The values of η were known from the ratio of the measured pellet rate to the rate at the surface, as calculated from Eq. (2) at the known T_s and $(C_{O_2})_s = (C_{O_2})_b$. Then the $\eta(\gamma_s, \beta_s, \phi_s)$ relations were used to evaluate the effective diffusivity, the only unknown in Eqs. (3)–(5). The results, shown in Table 2, indicate that the data were reproducible from pellet to pellet except for the values at the intermediate temperature level. At this temperature, the values of ϕ_s are in the intermediate range, where, with significant values of β_s and γ_s the effectiveness factor is large and very sensitive to ϕ_s . In extreme cases instabilities can occur (7). It is hypothesized that the variations in η at this temperature level are

TABLE 2
EFFECTIVE DIFFUSIVITY FOR UNIFORM PELLETS^a

Pellet no.	Temperature (°C)			Mole fraction O ₂		Pellet rate × 10 ⁶ (moles H ₂ O/(sec)(g))	Eff. factor (η)	Eff. diffusivity (D _e , cm ² /sec)	Tortuosity factor
	Bath	Surface	Center	y ₁	y ₀				
1	94	96.5	102.4	0.020	0.0133	2.34	0.99	0.16	2.4
	105.8	110.2	115.8	0.020	0.0115	2.97	1.11		
	140	147	152	0.020	0.0097	3.61	0.85	0.14	3.3
2	93	96	99	0.020	0.0132	2.28	0.98	0.15	2.6
	105	110	114	0.020	0.0114	2.89	1.07		
	140	147.5	151	0.020	0.0093	3.61	0.89	0.16	2.8
5	96	98	100	0.020	0.0132	2.38	0.98	0.15	2.6
	108	111	114	0.020	0.0112	3.08	1.15		
	143	144	150	0.020	0.0100	3.50	0.83	0.14	3.2

^a Flow rate, $F_t = 77$ cm³/min for pellets 1 and 5 and 74 cm³/min for pellet 2. The recirculation rate, $Q = 4000$ cm³/min. All rates are at 25°C and 1 atm.

due to the sensitivity of the effectiveness factor to small nonhomogeneities in catalyst particle concentration (in the inert Al_2O_3).

Effectiveness factors for the other two temperatures (Table 2) give consistent D_e values. The individual diffusivities corresponded to tortuosity factors from 2.4 to 3.3 as calculated from the expression

$$\delta_a = \frac{\bar{D}\epsilon_a}{D_e}, \quad (6)$$

where \bar{D} is a composite of bulk and Knudsen diffusivities for oxygen evaluated from

$$1/\bar{D} = (1/D_{O_2,H_2}) + (1/(\bar{D}_K)_{O_2}). \quad (7)$$

The Knudsen diffusivity was evaluated at the average macropore radius (Table 1). Since the catalyst particles were small and the pellet relatively large, it was assumed that the resistance to mass transfer in the micropores was negligible so that Eqs. (6) and (7) apply to the macropores. Tortuosity factors of this magnitude are expected for the macropore region of alumina pellets (6).

Mass Transfer Coefficient, k_m

The recirculation rate, Q , through the reactor was varied from 100 to 4000 cm^3/min , at two constant bath temperatures, 94 and 180°C, in order to investigate the effect on the rate of fluid-to-particle

mass transfer. These results, for which pellet No. 1 was used, are shown in Figs. 5 and 6. Since the curve in Fig. 5 is nearly horizontal it is concluded that the intrinsic rate at 94°C was so low that external mass transfer had a very small effect on the rate.

At 180°C (Fig. 6) the importance of mass transfer at low flow rates is evident, but at high flow rates the curve is again horizontal. Gas mixing is probably complete at high flow rates so that the measured outlet concentration of oxygen is the same as the bulk value in the reactor. Then the external mass transfer coefficient, k_m , can be calculated by writing Eq. (2) as

$$r_q = \eta_q(0.15)(p_{O_2})_s^{0.89} \exp\left(-\frac{5300}{R_g T_s}\right) \quad (8)$$

and employing the definition of k_m ,

$$r_q = 2k_m a_m \left(\frac{p}{R_g T}\right) (y_b - y_s)_{O_2}. \quad (9)$$

At any flow rate r_q , $(p_{O_2})_b$, and T_s are known. Then Eq. (8) and the $\eta(\gamma_s, \beta_s, \phi_s)$ relation, with Eqs. (3)–(5), provide the means to calculate $(C_{O_2})_s$ and η_q . With $(C_{O_2})_s$ known, k_m can be found from Eq. (9). The results for 180°C, which are approximate because the calculations are sensitive to small changes in r_q , give $k_m = 2.5$ cm/sec at $Q = 3000$ cm^3/min and 3.2 cm/sec at 4000 cm^3/min . Taking the area upon which to base the velocity as the void area in the reactor at the diameter of

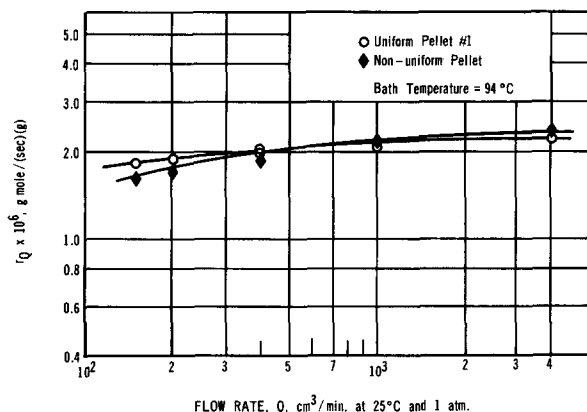


FIG. 5. Effect of flow rate on the rate of reaction; bath temperature = 94°C.

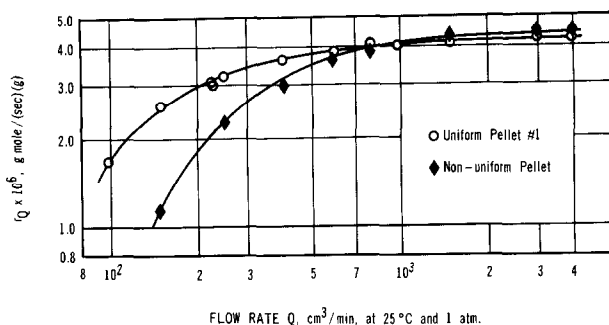


FIG. 6. Effect of flow rate on the rate of reaction; bath temperature = 180°C.

the pellet and the characteristic length as the pellet diameter, these values of Q correspond to Reynolds' numbers of 0.82 and 1.1, respectively. The flow system that approximates most closely our reactor arrangement, and for which mass transfer correlations are available, is perhaps that of flow past a single sphere. The minimum k_m corresponds to stagnant gas for which the Sherwood number, $k_m d_p / D_{O_2, H_2}$ is 2.0, or $k_m = 1.6$ cm/sec at 180°C. For Reynolds numbers in the range 0.8–1.1, the correlation given by Satterfield (6) leads to a nearly constant value of $k_m = 2.1$ cm/sec. The somewhat higher values from our calculations are probably due to the greater turbulence in the reactor in comparison with the turbulence associated with flow past a single sphere.

The Reynolds' numbers corresponding to Q from 100 to 4000 cm^3/min are low. Below 1000–2000 cm^3/min it seems likely that gas mixing is incomplete so that k_m varies with position around the pellet surface. Mass transfer coefficients could not be evaluated from our data at these low flow rates because the concentration of oxygen in the bulk gas was not uniform in the reactor and not equal to the measured value in the effluent stream.

NONUNIFORM PELLETS RESULTS

Rates of reaction vs flow rate for the nonuniform pellet are also shown in Figs. 5 and 6. At 94°C bath temperature the surface temperature was 2–4°C higher (4) for the nonuniform pellet than for the uniform

one. This perhaps explains why the rates in Fig. 5 are slightly higher for the nonuniform pellet at the highest flow rates. At the lowest flow rates the mass transfer retardation may be somewhat greater than the figure suggests because of this temperature difference. However, these small differences do not affect the conclusion that at 94°C external mass transport resistances are very small, even at flow rates less than 1000–2000 cm^3/min .

At 180°C bath temperature, the surface temperatures are 4–6°C higher for the nonuniform pellet. Hence, the effect of external mass transport is somewhat greater than suggested by a direct comparison of the low-flow rate region of the curves in Fig. 6. In any case the results show that at flow rates greater than 1000 cm^3/min (Reynolds No. = 0.27) external mass transfer does not affect reaction rate. The near coincidence of the curves for nonuniform and uniform pellets indicates that concentrating the active catalyst and reducing the mass transfer area to less than one-third does not change this conclusion. It is only for very low flow rates, where mixing is likely to be incomplete, that mass transfer resistance becomes important, and only then that the nonuniform pellet exhibits the greater mass transfer resistance. In other words the two curves in Fig. 6 become coincident and horizontal at about the same flow rate.

It should be noted that these conclusions apply only to a specific reaction system. A more active catalyst (higher

platinum content), or a greater reduction in mass transfer area, could give different results.

REFERENCES

1. Carslaw, H. S. and Jaeger, J. C., "Conduction of Heat in Solids," p. 233. Oxford, Clarendon Press, 1959.
2. Maymo, J. A. and Smith, J. M., *AIChE J.* **12**, 845 (1966).
3. Moffat, A. J., Johnson, M. M., and Clark, A., *J. Catal.* **18**, 345 (1970).
4. Patel, Kishor, "Site Localized Diffusion," M. S. thesis, Univ. of California, Davis, December, 1974.
5. Perry, J. H. (Ed.), "Chemical Engineers' Handbook." McGraw-Hill Book Company, New York, 1963.
6. Satterfield, C. N., "Mass Transfer in Heterogeneous Catalysis," p. 112, 157. M.I.T. Press, Cambridge, Mass., 1970.
7. Weisz, P. B. and Hicks, J. S., *Chem. Eng. Sci.* **17**, 265 (1962).